Published in final edited form as:
Int J Radiat Oncol Biol Phys. 2011 March 15; 79(4): 1188–1195. doi:10.1016/j.ijrobp.2010.10.007.

Hypofractionation results in reduced tumor cell kill compared to conventional fractionation for tumors with regions of hypoxia

David J. Carlson, Ph.D.[1,2], **Paul J. Keall, Ph.D.**[1], **Billy W. Loo Jr., M.D., Ph.D.**[1], **Zhe J. Chen, Ph.D.**[2], and **J. Martin Brown, Ph.D.**[1]

[1]Stanford University School of Medicine, Department of Radiation Oncology, Stanford, CA 94305-5847, USA

[2]Yale University School of Medicine, Department of Therapeutic Radiology, New Haven, CT 06520-8040, USA

Abstract

Purpose—Tumor hypoxia has been observed in many human cancers and is associated with treatment failure in radiation therapy. The purpose of this study is to quantify the effect of different radiation fractionation schemes on tumor cell killing assuming a realistic distribution of tumor oxygenation.

Method and Materials—A probability density function for the partial pressure of oxygen in a tumor cell population is quantified as a function of radial distance from the capillary wall. Corresponding hypoxia reduction factors (*HRFs*) for cell killing are determined. The surviving fraction of a tumor consisting of maximally resistant cells, cells at intermediate levels of hypoxia, and normoxic cells is calculated as a function of dose per fraction for an equivalent tumor biological effective dose under normoxic conditions.

Results—Increasing hypoxia as a function of distance from blood vessels results in a decrease in tumor cell killing for a typical radiotherapy fractionation scheme by a factor of 10^5 over a distance of 130 μ*m*. For head and neck and prostate cancer, the fraction of tumor clonogens killed over a full treatment course decreases by up to a factor of ~ 10^3 as the dose per fraction is increased from 2 to 24 Gy and from 2 to 18 Gy, respectively.

Conclusion—Hypofractionation of a radiotherapy regimen can result in a significant decrease in tumor cell killing compared to standard fractionation as a result of tumor hypoxia. There is a potential for large errors when calculating alternate fractionations using formalisms that do not account for tumor hypoxia.

Keywords

hypoxia; hypofractionation; LQ; cell survival; radiosensitizer

Corresponding Author: David J. Carlson, Ph.D. Yale University School of Medicine Department of Therapeutic Radiology New Haven, Connecticut 06520-8040 Tel: 203-200-2018 Fax: 203-688-8682 david.j.carlson@yale.edu.

Conflict of Interest Notification: none

INTRODUCTION

Tumor hypoxia has been observed in many human cancers and has been shown to correlate with treatment failure in radiation therapy (1). Approximately 90% of all solid tumors have median oxygen concentrations less than the typical values of 40–60 mmHg found in normal tissues (2). The decreased oxygenation of tumor cells is a result of structural and functional disturbances of the tumor vasculature which inhibit the normal delivery of oxygen (3). While hypoxia has been shown to be associated with increased metastasis (4), treatment failure in radiotherapy for tumors with high levels of hypoxia can be attributed primarily to the decreased sensitivity of hypoxic tumor cells to ionizing radiation (5).

The problem of hypoxic radioresistance is reduced through fractionation of the total radiation dose by reoxygenation (6). While emerging technologies such as stereotactic body radiotherapy (SBRT) provide valuable physical advantages over conventional radiation therapy for patients with solitary tumors (7,8), hypoxia is expected to be a significant mechanism of radioresistance in SBRT because the total radiation dose is delivered in only a few fractions and the potential for reoxygenation between fractions is reduced.

The purpose of this study is to quantify the effect of radiation fractionation on tumor cell killing assuming a realistic distribution of tumor oxygenation and full reoxygenation between fractions. Sensitivity of the results to variations in the radiobiologically hypoxic fraction, dose per fraction, and tumor intrinsic radiosensitivity is evaluated. The potential gain in cell killing through administration of a hypoxic cell radiosensitizer is also investigated.

METHODS AND MATERIALS

Development of a cell survival formalism that accounts for a realistic distribution of tumor hypoxia and the temporal pattern of radiation delivery

The distribution of oxygen in a tumor can be modeled using an arrangement of straight capillaries surrounded by viable tumor cells (9). Oxygen partial pressure $p(r)$ is expressed as a function of radial distance r from the capillary wall (10):

$$p(r) = p_0 \frac{R_{max}^2}{R_0^2} \left(2\ln\frac{R_{max}}{r} - 1 + \frac{r^2}{R_{max}^2} \right), \quad (1)$$

where p_0 is the initial oxygen partial pressure adjacent to the capillary wall and R_{max} is the diffusion limit of oxygen in tissue. The parameter R_0 is a constant related to the rates of oxygen consumption and diffusion:

$$R_0^2 = R_{max}^2 \left(2\ln\frac{R_{max}}{a} - 1 \right), \quad (2)$$

where the radius of the capillary a is assumed to be 10 μm.

As $p(r)$ decreases in a cell, the quantity of lethal radiation-induced damage formed through one- and two-track processes is decreased by a constant and by the square of this constant, respectively. Carlson *et al*. (11) have shown that a single factor can be used to modify intrinsic radiosensitivity in the linear-quadratic (LQ) model. The fraction of cells at radial distance r from the capillary wall that survive a single fraction of radiation dose d may be written as:

$$S(d) = \exp\left(-\left[\alpha_A / HRF(p)\right] d - \left[\beta_A G(\lambda, t) / HRF(p)^2\right] d^2\right), \tag{3}$$

where α_A and β_A are aerobic radiosensitivity parameters. For low-LET radiation, α represents the quantity of lethally misrepaired and unrepaired double-strand breaks (DSBs) and β represents the quantity of lethal exchange-type chromosome aberrations formed through binary misrepair of two separate DSBs (12). The Lea-Catcheside dose protraction factor $G(\lambda,t)$ is dependent on the duration of a single fraction t and the rate of DSB repair $\lambda \equiv \ln(2)/\tau$, where τ is the DSB repair half-time (13). A hypoxia reduction factor *HRF* is introduced to quantify reductions in known radiosensitivity parameters α_A and β_A as the oxygen partial pressure in a tumor cell decreases. The *HRF* is defined as the ratio of the dose at a specific level of hypoxia to the dose under fully aerobic conditions to achieve equal cell killing and is predicted by

$$HRF(p) = \frac{mK + p(r)}{K + p(r)}, \tag{4}$$

where m is the maximum *HRF* and K is the oxygen partial pressure at which the *HRF* is half the maximum value.

In a tumor cell population, the fraction of cells at radial distance r from the capillary center is

$$f(r) = 2\pi r / \int_a^{R_{hyp}} 2\pi r dr, \tag{5}$$

where R_{hyp} is the diffusion distance at which cells become maximally resistant. The surviving fraction of cells characterized by radial oxygen diffusion S_{diff} can be expressed as

$$S_{diff} = \int_a^{R_{hyp}} f(r) S(r) dr, \tag{6}$$

where $S(r)$ is calculated using Eq. (3). The percentage of cells that survive a single fraction of radiation in a population of maximally resistant tumor cells, i.e., the hypoxic fraction f_{hyp}, and tumor cells at intermediate and full oxygen levels ($1-f_{hyp}$) is

$$S_{fraction} = f_{hyp} S_{hyp} + \left(1 - f_{hyp}\right) S_{diff}. \tag{7}$$

where S_{hyp} is the surviving fraction of maximally resistant cells predicted by Eq. (3) using the maximum *HRF*. The total surviving fraction of tumor cells for a treatment of n fractions is

$$S_{total} = \left(S_{fraction}\right)^n \left(f_{hyp} \exp\left[\gamma_{hyp}(T - T_k)\right] + \left(1 - f_{hyp}\right) \exp\left[\gamma_{diff}(T - T_k)\right]\right), \tag{8}$$

where $\gamma \equiv \ln(2)/T_d$ is the rate or cellular proliferation, T_d is the cell doubling time, T is total treatment duration, and T_k is the onset or lag-time to cellular proliferation. The formulation above implicitly assumes that full reoxygenation occurs between fractions because the total population of cells returns to the initial oxygen distribution after each fraction. Several

clinical studies (14) have observed a general increase in tumor oxygenation during conventional therapy. Such increases work in favor of conventional fractionation and are not relevant to SBRT with a single or a few large doses.

Co-administration of a hypoxic cell radiosensitizer

The radiosensitizing effect of misonidazole has been shown to be dependent on the administered drug concentration and the oxygen partial pressure of the cell population (15). A sensitizer enhancement ratio *SER* is introduced that is dependent on drug concentration *c* and *p*(*r*), so that the surviving fraction of cells for a single fraction becomes

$$S(d) = \exp\left(-\left[\alpha_A \cdot SER(c,p)/HRF(p)\right] d - \left[\beta_A G(\lambda,t) \cdot SER(c,p)^2/HRF(p)^2\right] d^2\right). \quad (9)$$

The *SER* separates the radiosensitizing effects of misonidazole and oxygen and is defined as the quotient of the drug enhancement ratio and the oxygen enhancement ratio *OER* at a known oxygen partial pressure. The *SER* is predicted by

$$SER(p) = \frac{xy + p(r)}{y + p(r)}, \quad (10)$$

where *x* is the maximum *SER* and *y* is the oxygen partial pressure at which the *SER* is equal to half of the maximum value.

Selection of tumor sites and studies performed

Clinical data demonstrating a presence of tumor hypoxia in head and neck (H&N) (16) and prostate cancer (17) makes these tumor sites ideal for this study. The surviving fraction of tumor clonogens is simulated as a function of distance from the blood vessel based on radiosensitivity parameters derived from clinical data and *HRF* values derived from *in vitro* data. The surviving fraction is estimated for an entire radiotherapy course as a function of total number of fractions. Corresponding doses per fraction are calculated to achieve an equivalent tumor biological effective dose (BED) using the standard LQ model without corrections for tumor hypoxia, intrafraction DSB repair, or clonogen repopulation. A conventional H&N cancer treatment of 30 fractions of 2.2 Gy yields a BED of 80.5 Gy for a radiosensitivity of $\alpha_A = 0.25\ \text{Gy}^{-1}$ and $(\alpha/\beta)_A = 10$ Gy (18,19). A conventional prostate cancer treatment of 39 fractions of 2.0 Gy yields a BED of 130 Gy for a radiosensitivity of $\alpha_A = 0.15\ \text{Gy}^{-1}$ and $(\alpha/\beta)_A = 3.0$ Gy (20,21). Assumed time-dependent parameters for H&N cancer ($\tau_{hyp} = 1.0$ h, $\tau_{diff} = 5.0$ h, $T_k = 21$ days, $T_{d_{hyp}} = 6$ days, $T_{d_{diff}} = 3$ days) and prostate cancer ($\tau_{hyp} = 0.5$ h, $\tau_{diff} = 2.5$ h, $T_k = 60$ days, $T_{d_{hyp}} = 84$ days, $T_{d_{diff}} = 42$ days) are based on the best available data in the literature (20,22–24). All simulations are performed in FORTRAN 95.

RESULTS

Figure 1 shows oxygen partial pressure as a function of radial distance from the center of a capillary as predicted by Eq. (1). The solid line represents the assumed oxygen diffusion parameters ($p_0 = 60$ mmHg, $R_{max} = 150$ μm) that are most consistent with those expected in human tumors (25). This set of parameters results in an average oxygen partial pressure of 6.9 mmHg assuming that 20% of the tumor cells are maximally resistant ($p < 0.5$ mmHg) and 80% of the tumor cells are either well-oxygenated ($p > 20$ mmHg) or at intermediate oxygen levels ($p = 0.5$–20 mmHg). The value of $p = 6.9$ mmHg is consistent with typical

median oxygen partial pressures of 3–5 mmHg and 10–15 mmHg reported for prostate (17) and H&N (16) cancers, respectively.

Figure 2 shows the expected decrease in cellular radiosensitivity as a function of oxygen partial pressure. *HRF* values derived from data reported by Ling *et al.* (15), Koch *et al.* (26), Whillans and Hunt (27), and Carlson *et al.* (11) are denoted by white triangles, black circles, white circles, and gray circles, respectively. Reported *OER* values (15,26,27) were transformed into *HRF* values by dividing the maximum *OER* by the *OER* for each level of oxygenation. The *HRF* is at its maximum for anoxic conditions with a value of 2.8 and decreases to unity as the cells approach normoxic conditions. The dotted line shows the oxygen partial pressure (p = 0.5 mmHg) below which cells are assumed to be maximally resistant, i.e., radiobiologically hypoxic (9). Eq. (4) with best fit parameters m = 2.8 and K = 1.5 is used to convert the probability density function of the partial pressure of oxygen into a continuous distribution of *HRF* values.

Figure 3 shows surviving fraction of tumor clonogens as a function of radial distance from the capillary center for conventional H&N and prostate cancer treatments. Predictions are calculated using Eq. (3), neglecting intrafraction DSB repair (G = 1), and the total number of fractions, i.e., $S(d)^n$. Our simulations predict that tumor cell killing decreases by a factor of ~ 10^5 over a radial distance of 130 μm assuming an oxygen partial pressure of 60 mmHg at the capillary wall. The surviving fraction increases from 4.7×10^{-9} to 4.1×10^{-4} for H&N cancer and from 1.0×10^{-8} to 1.5×10^{-3} for prostate cancer. This predicted trend is consistent with experimental data from mouse tumors that shows a loss in radiosensitivity with distance from blood vessels (28).

Figure 4 shows surviving fraction of H&N and prostate tumor clonogens for an entire course of radiotherapy as a function of number of fractions, neglecting intrafraction DSB repair (G = 1) and clonogen repopulation (γ = 0). The equivalence of each fractionation schedule is demonstrated by the isoeffect achieved under normoxic conditions (i.e., *HRF* = 1). Solid symbols show model predictions for hypoxic fractions of 10%, 20%, and 30%. Tumor hypoxia increases cell survival by a factor of ~ 10^3 for conventionally fractioned radiotherapy as shown in earlier modeling studies (9). Tumor cell survival increases by additional factors of ~ 6×10^2 and ~ 4×10^2 as the dose per fraction is increased from 1.7 Gy (n = 40) to 24 Gy (n = 1) and from 2.0 Gy (n = 40) to 18 Gy (n = 1) for H&N and prostate cancer, respectively. Figure 5 shows the individual and combined effects of tumor hypoxia, tumor cell repopulation, and intrafraction DSB repair on total surviving fraction. Clonogen repopulation is most significant for hyperfractionated H&N cancer and strongly depends on the assumed lag time. For T_k = 21 days, cell killing decreases by a factor of ~ 6×10^2 as the dose per fraction is decreased from 3.7 to 1.7 Gy. For single fraction treatments, cell killing may be overpredicted by up to a factor of 24 if intrafraction DSB repair is neglected.

Figure 6 shows the distribution of *SER* values for the hypoxic cell radiosensitizer misonidazole derived from published *in vitro* data (15). White triangles and gray circles represent estimates for misonidazole concentrations of 1.2 mM and 5.0 mM, respectively. The *SER* is maximum for anoxic conditions with values of 1.4 and 2.0 for 1.2 mM and 5.0 mM concentrations, respectively, and decreases to unity as the cells approach normoxic conditions. Figure 7 shows the surviving fraction of tumor clonogens for different combinations of misonidazole and radiation. Values are shown for the characteristic 1–5 fractions of SBRT treatments. The addition of a hypoxic cell radiosensitizer at high doses per fraction is shown to be a potential strategy to obtain similar or greater levels of cell killing than achieved with conventional fractionation. Misonidazole has a greater sensitizing effect for large doses per fraction because of the increased importance of the hypoxic fraction of cells.

DISCUSSION

In this paper, we have determined the magnitude of cell killing lost as a result of tumor hypoxia during hypofractionated radiotherapy. To examine this problem, we developed a model that accounts for variations in the distribution of tumor hypoxia, tumor intrinsic radiosensitivity, and changes in radiation dose fractionation. Wouters and Brown (9) have previously shown that cells at intermediate oxygen levels are responsible for determining tumor response in conventionally fractionated radiotherapy. We have extended their work to examine changes in dose fractionation. Our model predicts a loss of up to three logs of cell kill as the dose per fraction is increased from a conventional size (e.g., 2.0–2.2 Gy) to a large single fraction dose (e.g., 18.3–23.8 Gy). The observed decrease in cell killing with increasing dose per fraction is attributed to (1) changes in the effective radiosensitivity (α/β) of tumors with heterogeneous oxygenation, (2) a reduction in interfraction reoxygenation, and (3) an increased importance of maximally resistant cells (i.e., the hypoxic fraction) in determining overall dose response as the total dose is delivered in a fewer number of fractions. This result demonstrates a potential for large errors when calculating alternate fractionations using BED formalisms that do not explicitly account for tumor hypoxia.

Oxygen diffusion vs. a binary hypoxia model

Authors of previous modeling studies (11,29) assumed a binary hypoxia distribution in which cells are either anoxic or normoxic. The effect of hypoxia is then modeled using one or two constant factors that effectively decrease intrinsic radiosensitivity. Several groups (29) have assumed that the observed reduction in radiosensitivity due to hypoxia is dose range dependent, e.g., α_A and β_A are scaled by statistically independent factors HRF_α and $(HRF_\beta)^2$, respectively. Carlson *et al*. (11) proposed that mechanistic considerations support that $HRF_\alpha \cong HRF_\beta$ and found that a single factor was able to provide as good a statistical fit to several *in vitro* data sets as independent factors. This assumption is especially convenient when attempting to estimate radiosensitivity parameters and *HRF* factors from sparse clinical data.

Wouters and Brown (9) first quantified differences in cell survival based on a radial oxygen diffusion model and a conventional binary model. They concluded that it is essential to characterize the oxygenation status of tumors in a realistic way, i.e., a dose-response model for hypoxic tumors must include cells at intermediate oxygen levels. If a binary model were used in this study, estimates of cell killing would change by more than two orders of magnitude for conventionally fractionated treatments. As illustrated in figure 4, a conventional prostate treatment of 39 fractions results in a surviving fraction of 2.8×10^{-5} using a model based on radial oxygen diffusion ($f_{hyp} = 0.2$). A binary model predicts a surviving fraction of 9.2×10^{-8} under the same conditions. Diffusion and binary models result in similar predictions for a single fraction of 18.3 Gy (9.7×10^{-3} and 8.5×10^{-3}, respectively) because overall response is dominated by the hypoxic fraction of the tumor cell population. A binary hypoxia model would therefore *overpredict* the decrease in tumor cell killing expected in hypofractionated radiotherapy as a result of tumor hypoxia.

Strategies to overcome tumor hypoxia

Many strategies have been proposed to overcome and even exploit tumor hypoxia (3,30). Hypoxia-activated prodrugs have been developed to specifically target radiation-resistant hypoxic cells. Other strategies include hypoxia-selective gene therapy, the use of recombinant obligate anaerobic bacteria, and targeting HIF-1. Ling *et al*. (31) developed the concept of hypoxia dose boosting by proposing a biological tumor volume that could be given additional radiation dose intended to overcome hypoxic radioresistance. Many technical difficulties exist with this strategy, including recent evidence that the distribution

of hypoxia can change significantly throughout the treatment for certain patients (32). In contrast, the use of hypoxic cell radiosensitizers is simpler because they have no problems in diffusion to the most hypoxic cells and effectively sensitize all hypoxic cells, both chronic and acute, to radiation (33). Despite the complexities involved with current imaging technology, hypoxia imaging will be necessary to categorize patients into subpopulations and determine who will benefit the most and least from strategies aimed at overcoming tumor hypoxia.

The model presented in this work will aid in the temporal optimization of radiation delivery by establishing when the effects of hypoxia on cell survival are most severe. Our results suggest tumor hypoxia has the largest negative effect on cell survival below ~10 fractions and treatments with $n > 10$ may be most effective. Alternatively, co-administration of a hypoxic cell radiosensitizer can increase the effectiveness of hypofractionated radiotherapy to achieve the same or greater level of cell killing as conventional regimens. Hypoxic cell radiosensitizers are most effective when delivered with a single or a few large doses of radiation. An etanidazole concentration of 12 g/m^2 (tumor concentration of ~ 5 mM) combined with a fraction of 15–24 Gy has been shown to be well tolerated (34). The 5.0 mM data in figure 7 is included only to be illustrative because such a large concentration of misonidazole could only be tolerated at most once. Tepper *et al.* (35) found no benefit in overall survival using a misonidazole dose of 3.5 g/m2 in conjunction with IORT of 15–20 Gy to the pancreas. These misonidazole doses provided five- to ten-fold lower sensitizer concentrations than achieved with a 12 g/m^2 dose of etanidazole (36). The co-administration of a hypoxic cell radiosensitizer during SBRT may help achieve the maximum therapeutic gain for hypoxic tumors.

Model assumptions and limitations

Aerobic radiosensitivity parameters for H&N and prostate cancer are chosen based on a range of reported estimates and recommendations of AAPM Task Group 137 (18–21). These values are not meant to be interpreted as the only biologically plausible parameters as it is widely known that there is inter- and intra-patient variability in radiosensitivity. For example, reported mean estimates of α for H&N cancer have been shown to range from 0.12–0.38 Gy^{-1} (18). Reported point estimates of α/β for prostate cancer range from 0.5–8.3 Gy and 1.1–8.4 Gy for *in vivo* and *in vitro* data, respectively (20,37). If we assume $\alpha = 0.04$ Gy^{-1} and $\alpha/\beta = 1.5$ Gy for prostate cancer (38), cell survival increases by a factor of 4.6 as the dose per fraction is increased from 2.0 Gy ($n = 40$) to 15.6 Gy ($n = 1$). This reduction in cell killing is smaller than observed in figure 4 due to the atypically low α value and not as a result of the lower α/β ratio. A recent clinical trial (39) found an insignificant trend favoring a hyperfractionated arm compared to the standard fractionation for the treatment of prostate cancer. While these results may imply a higher α/β for prostate cancer or the potential influence of incomplete repair between fractions, an additional intriguing possibility is that the hyperfractionated arm may be slightly advantageous in the presence of tumor hypoxia.

A common view exists that cells in the hypoxic regions of tumors do not proliferate. Recent data (40) suggests that significant proliferation can exist in hypoxic regions. Assumed tumor cell doubling times span the range of reported clinical estimates (22–24) and are consistent with data that suggests cell proliferation may be decreased under hypoxic conditions, on average, by a factor of ~2 (40). A common assumption made in modeling studies is that intrafraction DSB repair is negligible in high dose rate radiotherapy. However, as the total dose is increased, intrafraction DSB repair becomes more significant (20). Explicit inclusion of intrafraction DSB repair is shown to further reduce the level of cell killing predicted at high dose. Assumed DSB repair rates are consistent with tumor-specific data (20) and evidence that DSB repair rates may increase under hypoxic conditions (41).

Many investigators question the applicability of the LQ model at high doses (42,43). While more sophisticated kinetic reaction rate models (44,45) may provide a better fit to experimental data at larger doses, the LQ is only an approximation and predictions begin to deviate above ~ 5 Gy (13). Guerrero and Li (42) have shown that the LQ can predict experimental survival data well up to ~ 10 Gy. Brenner (46) suggests that the LQ model is appropriate for doses up to ~ 15–18 Gy if used correctly. The LQ is likely appropriate for use in analyzing hypoxic cell survival data up to an even higher dose range since hypoxia essentially scales the survival curve along the dose axis by a factor of the *HRF*.

One final aspect of the use of large dose fractions is the possibility that tumor cell killing might be enhanced by rapid endothelial cell apoptosis in tumor vessels. Garcia-Barros *et al*. (47) have reported that vascular endothelial cell apoptosis occurs at doses greater than ~ 8–10 Gy. Recently published clinical data showing a high rate of short-term local control for patients with metastatic spinal cord tumors treated with large single doses has been attributed to this phenomenon (8). However, while this is an intriguing possibility, there is a need for more data both preclinical and clinical before it can be an accepted mechanism for the effect of high dose fractions (48).

CONCLUSION

Tumor hypoxia has a large negative effect on tumor cell killing even with conventional fractionation assuming full reoxygenation between fractions. The modeling studies presented in this work also suggest that hypofractionation of a radiotherapy regimen will result in a significant decrease in tumor cell killing compared to standard fractionation as a result of tumor hypoxia. Corrections for tumor cell repopulation are shown to increase the effectiveness of hypofractionated treatments compared to conventional treatments for rapidly proliferating cancers. Biologically optimal fractionation schedules must balance treatment gains associated with reducing tumor repopulation against the potential for a loss of treatment efficacy associated with tumor hypoxia and intrafraction DSB repair. There is potential for the introduction of large errors into calculations of alternate dose fractionations when using models that do not account for tumor hypoxia, cellular proliferation, and DSB repair.

Acknowledgments

Work supported in part by NIH grant P01 CA067166 (JMB) and American Cancer Society IRG-58-012-52 (DJC).

REFERENCES

1. Brizel DM, Sibley GS, Prosnitz LR, et al. Tumor hypoxia adversely affects the prognosis of carcinoma of the head and neck. Int J Radiat Oncol Biol Phys 1997;38:285–289. [PubMed: 9226314]
2. Brown JM. The hypoxic cell: a target for selective cancer therapy--eighteenth Bruce F. Cain Memorial Award lecture. Cancer Res 1999;59:5863–5870. [PubMed: 10606224]
3. Brown JM. Exploiting the hypoxic cancer cell: mechanisms and therapeutic strategies. Mol Med Today 2000;6:157–162. [PubMed: 10740254]
4. Hockel M, Schlenger K, Aral B, et al. Association between tumor hypoxia and malignant progression in advanced cancer of the uterine cervix. Cancer Res 1996;56:4509–4515. [PubMed: 8813149]
5. Nordsmark M, Bentzen SM, Rudat V, et al. Prognostic value of tumor oxygenation in 397 head and neck tumors after primary radiation therapy. An international multi-center study. Radiother Oncol 2005;77:18–24. [PubMed: 16098619]
6. Kallman RF. The phenomenon of reoxygenation and its implications for fractionated radiotherapy. Radiology 1972;105:135–142. [PubMed: 4506641]

7. Timmerman R, Papiez L, McGarry R, et al. Extracranial stereotactic radioablation: results of a phase I study in medically inoperable stage I non-small cell lung cancer. Chest 2003;124:1946–1955. [PubMed: 14605072]
8. Yamada Y, Bilsky MH, Lovelock DM, et al. High-dose, single-fraction image-guided intensity-modulated radiotherapy for metastatic spinal lesions. Int J Radiat Oncol Biol Phys 2008;71:484–490. [PubMed: 18234445]
9. Wouters BG, Brown JM. Cells at intermediate oxygen levels can be more important than the "hypoxic fraction" in determining tumor response to fractionated radiotherapy. Radiat Res 1997;147:541–550. [PubMed: 9146699]
10. Tannock IF. Oxygen diffusion and the distribution of cellular radiosensitivity in tumours. Br J Radiol 1972;45:515–524. [PubMed: 5067983]
11. Carlson DJ, Stewart RD, Semenenko VA. Effects of oxygen on intrinsic radiation sensitivity: A test of the relationship between aerobic and hypoxic linear-quadratic (LQ) model parameters. Med Phys 2006;33:3105–3115. [PubMed: 17022202]
12. Carlson DJ, Stewart RD, Semenenko VA, et al. Combined use of Monte Carlo DNA damage simulations and deterministic repair models to examine putative mechanisms of cell killing. Radiat Res 2008;169:447–459. [PubMed: 18363426]
13. Sachs RK, Hahnfeld P, Brenner DJ. The link between low-LET dose-response relations and the underlying kinetics of damage production/repair/misrepair. Int J Radiat Biol 1997;72:351–374. [PubMed: 9343102]
14. Bergsjo P, Evans JC. Oxygen tension of cervical carcinoma during the early phase of external irradiation. I. Measurements with a Clark micro electrode. Scand J Clin Lab Invest Suppl 1968;106:159–166. [PubMed: 5731702]
15. Ling CC, Michaels HB, Epp ER, et al. Interaction of misonidazole and oxygen in the radiosensitization of mammalian cells. Int J Radiat Oncol Biol Phys 1980;6:583–589. [PubMed: 7410133]
16. Le QT, Kovacs MS, Dorie MJ, et al. Comparison of the comet assay and the oxygen microelectrode for measuring tumor oxygenation in head-and-neck cancer patients. Int J Radiat Oncol Biol Phys 2003;56:375–383. [PubMed: 12738312]
17. Parker C, Milosevic M, Toi A, et al. Polarographic electrode study of tumor oxygenation in clinically localized prostate cancer. Int J Radiat Oncol Biol Phys 2004;58:750–757. [PubMed: 14967430]
18. Girinsky T, Lubin R, Pignon JP, et al. Predictive value of in vitro radiosensitivity parameters in head and neck cancers and cervical carcinomas: preliminary correlations with local control and overall survival. Int J Radiat Oncol Biol Phys 1993;25:3–7. [PubMed: 8416879]
19. Stuschke M, Thames HD. Fractionation sensitivities and dose-control relations of head and neck carcinomas: analysis of the randomized hyperfractionation trials. Radiother Oncol 1999;51:113–121. [PubMed: 10435801]
20. Carlson DJ, Stewart RD, Li XA, et al. Comparison of in vitro and in vivo alphabeta ratios for prostate cancer. Phys Med Biol 2004;49:4477–4491. [PubMed: 15552412]
21. Nath R, Bice WS, Butler WM, et al. AAPM recommendations on dose prescription and reporting methods for permanent interstitial brachytherapy for prostate cancer: report of Task Group 137. Med Phys 2009;36:5310–5322. [PubMed: 19994539]
22. Fowler JF. Optimum overall times II: Extended modelling for head and neck radiotherapy. Clin Oncol (R Coll Radiol) 2008;20:113–126. [PubMed: 18155893]
23. Dasu A, Fowler JF. Comments on "Comparison of in vitro and in vivo alphabeta ratios for prostate cancer". Phys Med Biol 2005;50:L1–4. author reply L5–8. [PubMed: 17001787]
24. Haustermans KM, Hofland I, Van Poppel H, et al. Cell kinetic measurements in prostate cancer. Int J Radiat Oncol Biol Phys 1997;37:1067–1070. [PubMed: 9169814]
25. Vaupel P, Fortmeyer HP, Runkel S, et al. Blood flow, oxygen consumption, and tissue oxygenation of human breast cancer xenografts in nude rats. Cancer Res 1987;47:3496–3503. [PubMed: 3581084]

26. Koch CJ, Stobbe CC, Bump EA. The effect on the Km for radiosensitization at 0 degree C of thiol depletion by diethylmaleate pretreatment: quantitative differences found using the radiation sensitizing agent misonidazole or oxygen. Radiat Res 1984;98:141–153. [PubMed: 6718689]
27. Whillans DW, Hunt JW. A rapid-mixing comparison of the mechanisms of radiosensitization by oxygen and misonidazole in CHO cells. Radiat Res 1982;90:126–141. [PubMed: 7038754]
28. Chaplin DJ, Durand RE, Olive PL. Cell selection from a murine tumour using the fluorescent probe Hoechst 33342. Br J Cancer 1985;51:569–572. [PubMed: 2579667]
29. Dasu A, Denekamp J. New insights into factors influencing the clinically relevant oxygen enhancement ratio. Radiother Oncol 1998;46:269–277. [PubMed: 9572620]
30. Brown JM, Wilson WR. Exploiting tumour hypoxia in cancer treatment. Nat Rev Cancer 2004;4:437–447. [PubMed: 15170446]
31. Ling CC, Humm J, Larson S, et al. Towards multidimensional radiotherapy (MD-CRT): biological imaging and biological conformality. Int J Radiat Oncol Biol Phys 2000;47:551–560. [PubMed: 10837935]
32. Lin Z, Mechalakos J, Nehmeh S, et al. The influence of changes in tumor hypoxia on dose-painting treatment plans based on 18F-FMISO positron emission tomography. Int J Radiat Oncol Biol Phys 2008;70:1219–1228. [PubMed: 18313529]
33. Brown JM. Keynote address: hypoxic cell radiosensitizers: where next? Int J Radiat Oncol Biol Phys 1989;16:987–993. [PubMed: 2649468]
34. Drzymala RE, Wasserman TH, Won M, et al. A phase I-B trial of the radiosensitizer: etanidazole (SR-2508) with radiosurgery for the treatment of recurrent previously irradiated primary brain tumors or brain metastases (RTOG Study 95-02). Radiother Oncol 2008;87:89–92. [PubMed: 18342381]
35. Tepper JE, Shipley WU, Warshaw AL, et al. The role of misonidazole combined with intraoperative radiation therapy in the treatment of pancreatic carcinoma. J Clin Oncol 1987;5:579–584. [PubMed: 3559650]
36. Halberg FE, Cosmatis D, Gunderson LL, et al. RTOG #89-06: a phase I study to evaluate intraoperative radiation therapy and the hypoxic cell sensitizer etanidazole in locally advanced malignancies. Int J Radiat Oncol Biol Phys 1994;28:201–206. [PubMed: 8270442]
37. Dasu A. Is the alpha/beta value for prostate tumours low enough to be safely used in clinical trials? Clin Oncol (R Coll Radiol) 2007;19:289–301. [PubMed: 17517328]
38. Brenner DJ, Hall EJ. Fractionation and protraction for radiotherapy of prostate carcinoma. Int J Radiat Oncol Biol Phys 1999;43:1095–1101. [PubMed: 10192361]
39. Valdagni R, Italia C, Montanaro P, et al. Is the alpha-beta ratio of prostate cancer really low? A prospective, non-randomized trial comparing standard and hyperfractionated conformal radiation therapy. Radiother Oncol 2005;75:74–82. [PubMed: 15878104]
40. Hoskin PJ, Sibtain A, Daley FM, et al. The immunohistochemical assessment of hypoxia, vascularity and proliferation in bladder carcinoma. Radiother Oncol 2004;72:159–168. [PubMed: 15297134]
41. Frankenburg-Schwager M, Harbich R, Beckonert S, et al. Half-life values for DNA double-strand break rejoining in yeast can vary by more than an order of magnitude depending on the irradiation conditions. Int J Radiat Biol 1994;66:543–547. [PubMed: 7983443]
42. Guerrero M, Li XA. Extending the linear-quadratic model for large fraction doses pertinent to stereotactic radiotherapy. Phys Med Biol 2004;49:4825–4835. [PubMed: 15566178]
43. Park C, Papiez L, Zhang S, et al. Universal survival curve and single fraction equivalent dose: useful tools in understanding potency of ablative radiotherapy. Int J Radiat Oncol Biol Phys 2008;70:847–852. [PubMed: 18262098]
44. Curtis SB. Lethal and potentially lethal lesions induced by radiation--a unified repair model. Radiat Res 1986;106:252–270. [PubMed: 3704115]
45. Tobias CA. The repair-misrepair model in radiobiology: comparison to other models. Radiat Res Suppl 1985;8:S77–95. [PubMed: 3867092]
46. Brenner DJ. The linear-quadratic model is an appropriate methodology for determining isoeffective doses at large doses per fraction. Semin Radiat Oncol 2008;18:234–239. [PubMed: 18725109]

47. Garcia-Barros M, Paris F, Cordon-Cardo C, et al. Tumor response to radiotherapy regulated by endothelial cell apoptosis. Science 2003;300:1155–1159. [PubMed: 12750523]

48. Brown JM, Koong AC. High-dose single-fraction radiotherapy: exploiting a new biology? Int J Radiat Oncol Biol Phys 2008;71:324–325. [PubMed: 18474308]

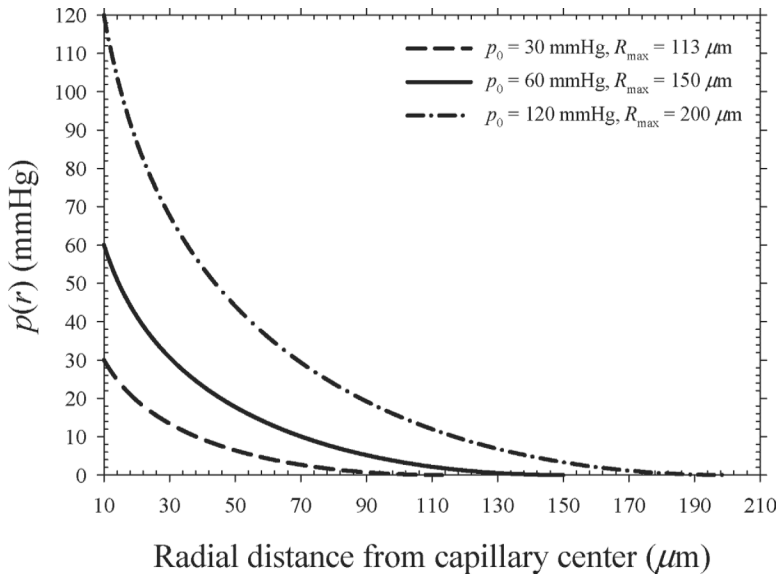

Figure 1.
Oxygen partial pressure as a function of radial distance from the center of a capillary. The solid line represents the assumed oxygen diffusion parameters that result in an average oxygen partial pressure of ~ 6.9 mmHg.

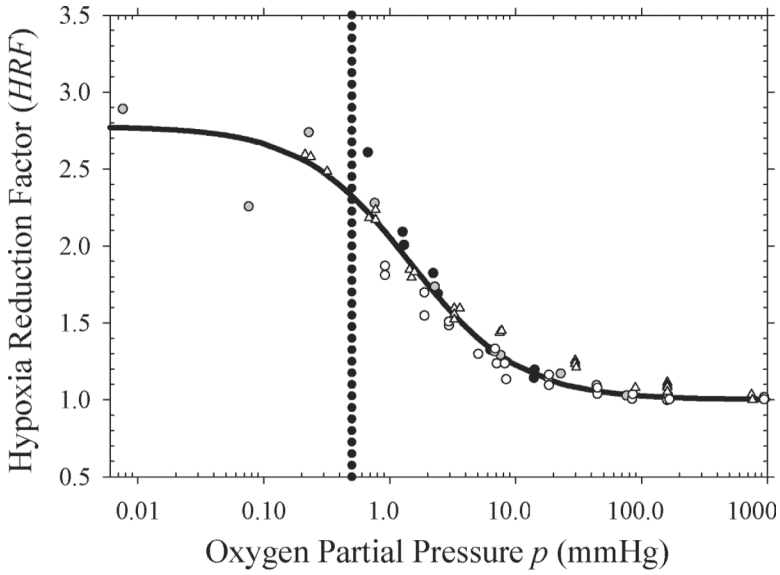

Figure 2.
Hypoxia reduction factor (*HRF*) values derived from published cell survival data (11,15,26,27). Solid line shows a fit to the values using Eq. (4) with $m = 2.8$ and $K = 1.5$.

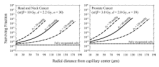

Figure 3.
Surviving fraction of tumor clonogens as a function of radial distance from the capillary center for conventional radiotherapy fractionations.

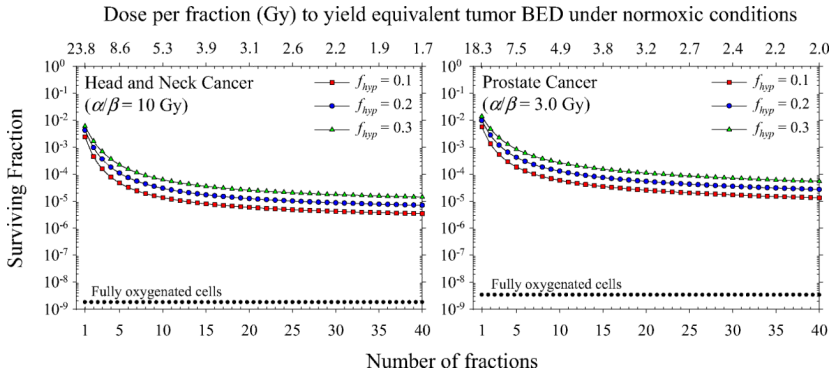

Figure 4.

Total surviving fraction of tumor clonogens as a function of dose per fraction assuming daily fractionation and full reoxygenation between fractions. Dependence of model predictions on the assumed value of the hypoxic fraction of cells is shown.

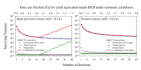

Figure 5.
Total surviving fraction of tumor clonogens as a function of dose per fraction assuming daily fractionation and full reoxygenation between fractions. Dependence of model predictions on intrafraction DSB repair and clonogen repopulation is shown.

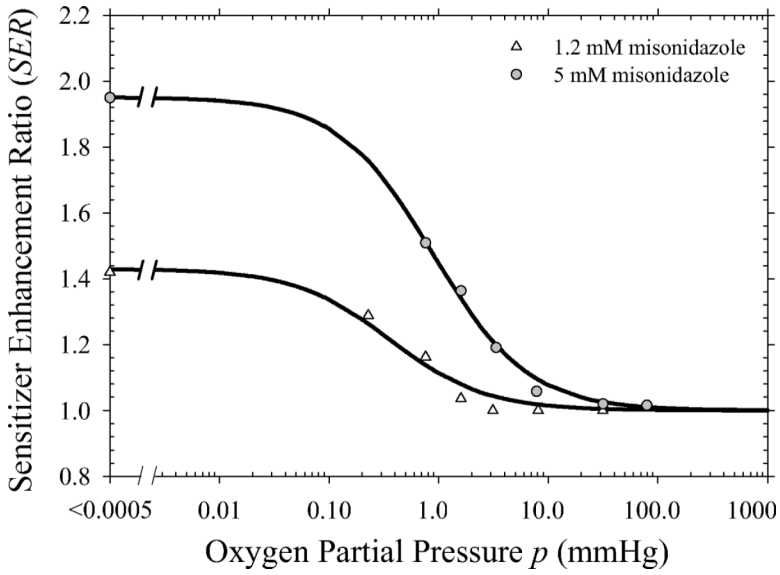

Figure 6.

Sensitizer enhancements ratio (*SER*) values derived from published cell survival data (15). Solid lines shows a fit to the values using Eq. (10) with $x = 1.4$ and $y = 0.4$ for the 1.2 mM concentration and $x = 2.0$ and $y = 0.9$ for the 5.0 mM concentration.

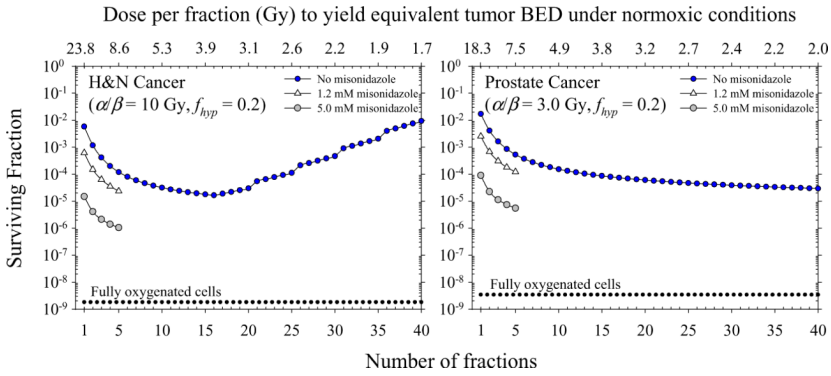

Figure 7.

Effect of misonidazole and radiation on surviving fraction of tumor clonogens assuming a realistic distribution of tumor hypoxia, intrafraction DSB repair, and clonogen repopulation. Dotted lines show predictions neglecting corrections for hypoxia, repair, and repopulation.